Phase-coherent multichannel SDR - Sparse array beamforming

Mikko Laakso Robin Rajamäki Risto Wichman Visa Koivunen

Department of Signal Processing and Acoustics, Aalto University, mikko.t.laakso@aalto.fi,
firstname.lastname@aalto.fi

Abstract

In this paper, a modular and inexpensive coherent multichannel software-defined radio receiver is introduced and direction-of-arrival (DOA) estimation is performed, comparing the results between the full and sparse arrays. Sparse sensor arrays can reach the resolution of a fully populated array with reduced number of elements, which relaxes the required structural complexity of e.g. antenna arrays and RF front-ends. Results from the collected data set are analyzed with the widely known DOA estimator Multiple Signal Classification (MUSIC). Generally, the sparse array estimates agree with the full array, except when strong interfering reflections are present, as expected.

1 An inexpensive phase-coherent multichannel SDR receiver

Commercial phase-coherent multichannel solutions are often prohibitively expensive for low-budget research. A paragon of such commercial system is the Lund University Massive MIMO testbed [1]. Affordability was the main motivation for designing the multichannel platform based on the inexpensive RTL-SDR receiver. The RTL-SDR, originally an USB DVB-T tuner, supports sample rates up to 2.56 MHz and gives access to a stream of 8-bit quadrature samples. Compared to the Ettus Research USRP radios used by Malkowsky et al. in [1], the RTL-SDR bandwidth is modest and the system does not have transmit capability. A brief description of the coherent system is given below, for more information, see [2].

The coherent receiver is based on an array of RTL-SDR receivers, all driven by a common clock signal and connected to a switchable reference noise generator, as visualized in Fig 1. The signal receivers are housed in a coupler module, built on top of an USB hub, which accommodates 7 RTL-SDR receivers. A dedicated reference receiver records only the reference noise, sample vector $\mathbf{r}$, which is generated with a reverse-biased Zener-diode. The same noise is distributed to the signal receivers with directional couplers on the antenna lines of the custom-built coupler circuit board. This enables aligning the signal sample streams in time and phase with cross-correlation. We simply find the maximum of the cross-correlation estimate $|\hat{\phi}_{\mathbf{x_n r}}(l)|$ for each signal vector $\mathbf{x}$. To limit the computational load on the host computer doing the processing, shifting the signal stream timing is performed by adjusting the RTL-SDR hardware resampler, originally intended to correct carrier frequency offsets. To further lighten the processing load, the correlation calculation is switched off once a given signal channel is deemed time synchronized.

As opposed to the sampling clock which all the receivers obtain from a common source seen in Fig 1, the tuner RF oscillator is derived from this common clock via PLL frequency synthesis. The PLL acquires lock in an arbitrary phase, therefore the phase needs to be calibrated whenever the receiver is retuned. It was also observed that the relative phases of the signal streams drift slowly during constant operation. Fortunately, the rate of this drift is typically less than 1° per minute. Therefore, before each measurement, we calculate a phase-correction coefficient α_n for all signal channels 1 to n with $\alpha_n = \langle \mathbf{x_n}^*, \mathbf{r} \rangle / |\langle \mathbf{x_n}^*, \mathbf{r} \rangle|$. Coefficient α_n is averaged over a few frames to reduce noise and then the corrected receiver phase is assumed coherent for the duration of the measurement.

The reference noise is enabled only during the time synchronization and calculation of the phasors α, otherwise it dramatically degrades signal-to-noise ratio (SNR). Furthermore, the noise

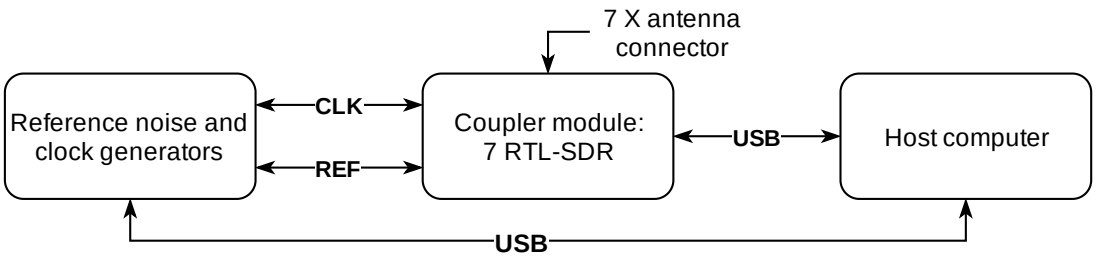

Fig. 1: Block diagram of a receiver system with one coupler module.

is by design highly correlated and relatively strong across the signal channels, which is problematic for DOA techniques. Were it not switched off, a DOA estimate would show a strong signal impinging from 0°, directly towards the broadside of the antenna.

2 Sparse array beamforming

A sparse sensor array achieves the same aperture as a full array with a reduced number of elements. Only a brief description of the idea is given below, for more information, refer to for instance [3]. The *sparse array*, is typically approached through a virtual co-array of element sums or differences [3]. In most cases, the physical distance between the array elements is half wavelength, $\lambda/2$, and the array is hereafter described in integer d multiples of this distance. Consider a contiguous linear array with N equispaced elements, with an aperture of $L = N-1$. Let $\mathcal{D} = \{0, 1, \ldots, N-1\}$ be the set of normalized element distances, $|\mathcal{D}| = N$, then the difference co-array $\mathcal{D}_\Delta$ is [3]:

$$\mathcal{D}_\Delta = \{d_j - d_k \mid d \in \mathcal{D}\} \quad j,k = 0,1,...,N-1. \tag{1}$$

With increasing N, the redundancy in (1) increases, i.e. $d_j - d_k$ above yield multiple identical differences. A fully populated linear array with $N \geq 3$ always has a redundant co-array.

When the array is sparse, $\mathcal{D}$ is not a contiguous set of integers and the array is said to contain holes. Certain geometries can still represent the contiguous set of integers $\{0, 1, \ldots, L\}$ with the co-array (1). However, it is known that any sparse array with $N > 4$ has a redundant co-array [4]. A Minimum-redundancy array (MRA) minimizes $|\mathcal{D}|$ such that $\mathcal{D}_\Delta = \{0, 1, \ldots, L\}$, that is, finds an array geometry with the smallest number of elements that can still produce a fully populated co-array. Fig. 2 shows an example of an MRA with $N = 4$ and a uniform linear array (ULA) with $N = 7$ elements. The two arrays achieve the same aperture $L = 6$. A sparse ruler analogy is often used in explaining the sparse array, and turns out this problem is closely related to the concept of Golomb rulers researched in the field of number theory, also discussed in [4]. A closed-form solution for finding minimum-redundancy array geometries is not known and the search for such optimal geometries for large N is a computationally hard combinatorial problem [3].

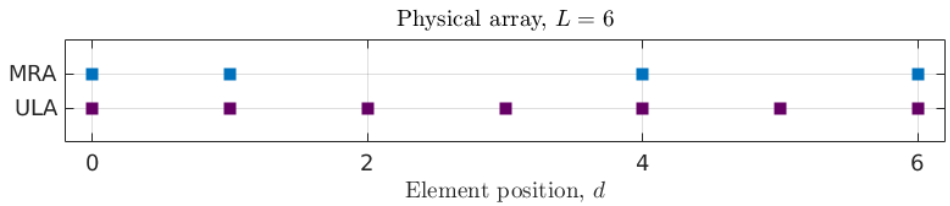

Fig. 2: Array configuration

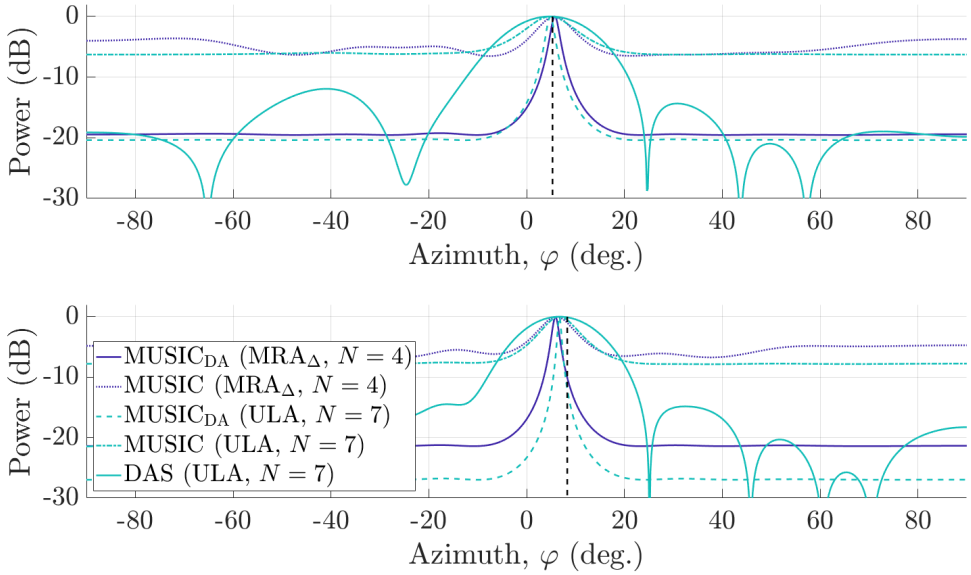

Fig. 3: ULA and MRA spatial spectrums, with and without DAA. Dashed vertical line represents the true location of the source.

We use the well-known MUSIC algorithm for DOA estimation, for which the spatial spectrum power as a function of source angle ϕ reads

$$P_{music}(\phi) = \frac{1}{\mathbf{s}^{\dagger}(\phi)\mathbf{Q_n}\mathbf{Q_n}^{\dagger}\mathbf{s}(\phi)} \tag{2}$$

where $\dagger$ denotes the Hermitian transpose, $\mathbf{s}$ is the array steering vector and $\mathbf{Q_n}$ is the noise subspace from the full eigenvalue decomposition of the covariance matrix, i.e. $\mathbf{R_{SS}} = \mathbf{Q}\Lambda\mathbf{Q}^{\dagger} = \mathbf{Q_s}\Lambda_{\mathrm{s}}\mathbf{Q_s}^{\dagger} + \mathbf{Q_n}\Lambda_{\mathrm{n}}\mathbf{Q_n}^{\dagger}$ [5]. For eigenspace methods such as MUSIC, which operate on the estimated signal covariance matrices, the $\mathbb{C}^{(L+1)\times(L+1)}$ matrix $\mathbf{R_{SS}}$ can be directly expanded from the estimated $\mathbb{C}^{N\times N}$ sparse array covariance matrix. One such method is *direct augmentation* (DAA), introduced by Pillai et al. in [6]. DAA imposes a Toeplitz structure and imputes the missing spatial correlations using the corresponding lags from $\mathcal{D}_{\Delta}$. Averaging can be employed for redundant lags. However, the resulting augmented $\mathbf{R_{SS}}$ is not anymore guaranteed to be positive definite [7]. This has implications in scenarios where e.g. the number of signal sources is not known a priori and is to be estimated from eigenvalue magnitudes. Finally, co-array based DOA has also been experimentally verified to be sensitive to multipath propagation [8].

3 Results and conclusions

An informal series of measurements was conducted in a typical office room environment, on the development version of the receiver described in Section 1. The walls of the room are concrete and assumed to cause substantial reflections. The receiver is connected to an $N = 9$ ULA of monopole antennas with an inter-element distance of 0.125 m. The transmitter, at a distance of approximately 3 m, is configured to send a carrier wave on frequency of 1240 MHz. The receiver records the sample data for all 9 channels at a sample rate of 1 MHz. Altogether 13 frames of 81920 samples are collected, moving the signal source a distance corresponding to approximately 1.5° change in direction between the frames. Data from two channels belonging to antennas at a close distance (15 cm) from an adjacent wall had to be discarded due to interfering reflections.

The spatial spectrums in Fig. 3 were computed with and without direct augmentation for both ULA and MRA cases. A delay-and-sum (DAS) beamformer is also included as a reference. In most collected frames, the DOA estimate tracks the signal source correctly. In Fig. 3 top, the DOA estimate correspondence is almost spot on, whereas the bottom plot represents one of the worst cases where the error is 2.5°. Finally, co-array processing with DAA is also tested on the full ULA array and clearly extends the dynamic range, which is pronounced in Fig. 3 bottom.

Evidently, the phase-coherence of the receiver holds since the DOA estimates are reasonable. Furthermore, the estimates from the thinned array agree with the full array. More data will be needed and measurements in open space are under way.

References

[1] S. Malkowsky et al., "The World's First Real-Time Testbed for Massive MIMO: Design, Implementation and Validation," in *IEEE Access*, vol. 5, pp. 9073-9088, 2017.

[2] M. Laakso, "Multichannel coherent receiver on the RTL-SDR," M.S. Thesis, Sch. of Electrical Engineering, Aalto Univ., Espoo, 2019. Available: `https://aaltodoc.aalto.fi/handle/123456789/37163`

[3] R. Rajamäki and V. Koivunen, "Comparison of Sparse Sensor Array Configurations with Constrained Aperture for Passive Sensing," *2017 IEEE Radar Conference (RadarConf),* Seattle, WA, 2017, pp. 0797-0802.

[4] D. A. Linebarger, I. H. Sudborough and I. G. Tollis, "Difference bases and sparse sensor arrays," *IEEE Transactions on Information Theory,* vol. 39, no. 2, pp. 716-721, Mar. 1993.

[5] R. Schmidt, "Multiple emitter location and signal parameter estimation," *IEEE Transactions on Antennas and Propagation,* vol.34, no.3, pp.276-280, Mar. 1986.

[6] S. Pillai, F. Haber and Y. Bar-Ness, "A new approach to array geometry for improved spatial spectrum estimation," *ICASSP '85. IEEE International Converence on Acoustics, Speech, and Signal Processing,* Tampa, FL, USA, 1985, pp. 1816-1819.

[7] Y. I. Abramovich, D. A. Gray, A. Y. Gorokhov and N. K. Spencer, "Positive-definite Toeplitz completion in DOA estimation for nonuniform linear antenna arrays. I. Fully augmentable arrays," *IEEE Transactions on Signal Processing,* vol. 46, no. 9, pp. 2458-2471, Sept. 1998.

[8] J. Wang, H. Xu, G. J. T. Leus and G. A. E. Vandenbosch, "Experimental Assessment of the Coarray Concept for DoA Estimation in Wireless Communications," *IEEE Transactions on Antennas and Propagation,* vol. 66, no. 6, pp. 3064-3075, June 2018.